

# Symplectic and antiplectic waves in an array of beating cilia attached to a closed body

Aref Ghorbani<sup>1</sup> and Ali Najafi<sup>1,2</sup>

<sup>1</sup>*Department of Physics, Institute for Advanced Studies in Basic Sciences (IASBS), Zanjan 45137-66731, Iran*

<sup>2</sup>*Physics Department, University of Zanjan, Zanjan 313, Iran\**

(Dated: August 11, 2018)

By taking into account the hydrodynamic interactions in a one dimensional array of model cilia attached to a no-slip cylindrical surface, we investigate their synchronized motion. We show, how does the emergence of metachronal waves depend on the initial state of the system and investigate the conditions under which, the formation of symplectic and antiplectic waves are possible.

PACS numbers: 47.63.Gd, 87.16.Qp, 05.45.Xt

## I. INTRODUCTION

Cillium, a micron scale flexible hair-like appendix and their ensembles appear in many biological systems[1]. Mucociliary transport in respiratory system and swimming of ciliated organisms like Volvox and Paramecium are among the most important examples of cilia in biology [2–6]. Using the forces from molecular motor-proteins embeded in its molecular structure, an individual cilium can beat and produce flow field [7]. In most of their natural appearance, the emergent synchronized motion in the form of metachronal wave developed in assemblies of cilia is an essential key in their performance. This is due to the fact that the flow field corresponding to an individual cilium is negligibly small but a synchronized pattern of ciliary beating is able to either produce a net flow of fluid in mucus or generate a swimming mechanism for the ciliated microorganisms. The metachronal wave is a kind of synchronized pattern of ciliary beating that results a traveling wave on the envelop of their tips. Experimental studies show that the direction of a metachronal wave can be either parallel (symplectic wave) or antiparallel (antiplectic wave) to the direction of power-stroke in an individual cilia [5, 8]. Physical mechanism behind this wave pattern formation is not completely understood but it is mainly believed that the hydrodynamic interactions between cilia, can lead their assembly to reach a synchronized state with propagating metachronal waves [9–11]. There are some experimental observations in artificial active colloidal systems that support the idea of hydrodynamic mediated synchronization in colloidal systems[12–15]. In addition to the hydrodynamic interactions, new studies have suggested that precise coordination of flagellar motion is provided by contractile fibers of the basal membrane [16]. In most of recent works a flat geometry for the basal ciliated mebrane has been considered [17–23]. Motivated from the hydrodynamic effects due to a rough wall [24], one can expect to see the effects due to the curvature of a ciliated body in the synchronization of its cilia. In a very recent study, the synchronization of cilia attached to a sphere has been addressed and it is

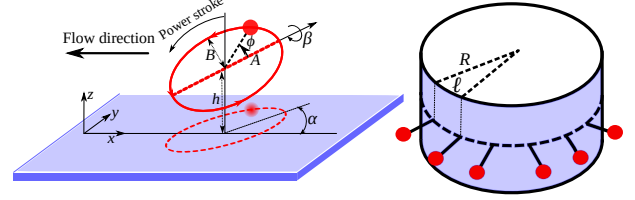


FIG. 1. Left: geometry of a single cilium, right: an array of cilia attached to the surface of a cylinder. The direction of power stroke and the average flow are shown in figure.

shown that metachronal waves can appear [25]. In this article we revisit the emergence of metachronal waves on a curved ciliated body and consider a ring of cilia attached to the peripheral of a cylindrically curved body. Following the model of Vilfan *et al.*, we consider each cilium as a small sphere moving along an elliptic trajectory [17]. To take into account the effect of curvature in the hydrodynamic interaction, we use an approximate scheme and assume that the interaction of two adjacent cilia can be calculated using a flat wall that is locally tangent to the surface. We will show that as a result of asymmetry in the orbit, both symplectic and antiplectic waves can emerge.

## II. MODEL

In order to study the motion of an assembly of cilia, we start by defining our simplified mechanical model for a single cilium. To simplify the motion, instead of considering the dynamics of a real cilium which has many degrees of freedom, we can consider the motion of its center of mass. Fluid flow produced by a small sphere located at the position of center of mass resembles the flow pattern due to the cilium. Regarding the periodic motion of a cilium, the sphere should move on a closed trajectory. Fig. 1-left, mimics the trajectory on which the cilium center of mass moves. Verified by experiments, the ciliary cycle is asymmetric so the friction forces are different for the first and second half of the cycle. These half cycles compose the power stroke and the recovery. This asymmetry that should be reflected in the trajec-

\* najafi@iasbs.ac.ir

tory, is essential in allowing the cilium to produce a net flow of fluid along its stroke direction. In determining the dynamics and also the shape of the trajectory, one should consider the experimental fact that a cilium has a self sustained dynamics. As a result of this self sustained motion the phase variable, angle of the motion along the trajectory, is free. This phase freedom is essential in synchronization of two cilia. Considering this phase freedom, two classes of models can be considered. In the first class of models it is assumed that the trajectory is on average a circular path. This means that the internal forces of molecular motors can be divided into two parts: a constant tangential force along the preferred trajectory and an elastic radial restoring force that guarantees an average finite radius for the trajectory [25, 26]. Such radial elastic force allows the system to behave like a phase-free rotator.

In the second class of models, instead of fixing a value for the tangential force, its response function, a relation between the force and velocity, has been considered. In this article, we will use this kind of modeling to consider the dynamics of cilia [17, 27]. Schematic view of the model and its geometrical parameters are shown in fig. 1(left). In a reference frame located on the wall (Lab. frame), the sphere moves on an elliptic orbit that is characterized by 6 parameters,  $A$ ,  $B$ ,  $h$ ,  $x$ ,  $\alpha$  and  $\beta$ . The lengths of semi-major and semi-minor axes are denoted by  $A$  and  $B$  and the position vector of the center of ellipse is given by  $(x, 0, h)$ . A rigid wall stands for the body is placed at  $z = 0$ . The plane of the ellipse and the rigid wall are not parallel, the plane of ellipse is rotated with an angle  $\beta$  around its semi-major axis. Projecting the orbit on the plane, the semi-major axis is tilted with an angle  $\alpha$  with respect to  $x$ -axis. For later use we denote the eccentricity of the orbit by  $e = \sqrt{1 - (\frac{B}{A})^2}$ . Instantaneous dynamical state of the sphere moving on this orbit, is denoted by an angle  $\phi(t)$ . In the laboratory frame, the instantaneous position vector for a cilium that depends on time only through the phase variable  $\phi(t)$  can be written as:

$$\mathbf{r}[\phi(t)] = \begin{bmatrix} x \\ 0 \\ h \end{bmatrix} + \mathcal{R}_A(\beta)\mathcal{R}_z(\alpha) \begin{bmatrix} A \cos \phi \\ B \sin \phi \\ 0 \end{bmatrix},$$

where  $\mathcal{R}_z(\alpha)$  and  $\mathcal{R}_A(\beta)$  denote the rotation matrices around  $z$  and major axis of the ellipse. In this article we use columnar matrices to show the vectors.

Based on an intuitional argument, we can easily distinguish the direction of average flow produced by a cilium. It is essential to note that only a tilted elliptic trajectory ( $\beta \neq 0$ ) is able to produce net flow. For a tilted trajectory, we can decompose the ciliary cycle into two sub-trajectories both parallel to the wall, one near and the other far from the wall. The cilium has more or less the same velocity in both parts but the friction coefficient is greater in the near wall case. As a result of smaller friction coefficient, the force exerted on fluid is

stronger at the part that is far from wall. This means that the motion of cilium in a part of its trajectory that is far from the wall, determines the flow direction. Thus the flow pattern is in the same direction as the cilium moves in its motion where it is far from wall. For a typical trajectory shown in fig. 1(left), the direction of the flow points from right to left. In this argument we have neglected the parts of trajectory that are perpendicular to the wall, such parts will have contribution in flow perpendicular to the wall. In the case of many coordinated cilia, the perpendicular part of the velocity profile averages to zero.

In this article we aim to investigate the curvature of the ciliated body and its role in the dynamic of cilia. In order to attack this problem, we consider a 1 dimensional array of  $\mathcal{N}$  cilia attached to a circle around the cylinder. The circle is wrapped around the cylinder and it has the same radius  $R$  as cylinder. As shown in fig. 1(right), two adjacent cilia are connected with an arc length  $\ell = 2\pi R/\mathcal{N}$ . The geometrical parameters of each cilia can be expressed with respect to a flat wall that is locally tangent to the cylinder. In the case that the length of each cilium, is comparable with this arc-length, we expect to see hydrodynamical effects due to the curvature of body. In the next section we will summarize all of the equations that are necessary to describe the dynamics of a coupled system of cilia.

### III. DYNAMICAL EQUATIONS

Let us consider two cilia, each represented by a moving sphere with radii  $a$  and position vectors given by  $\mathbf{r}_i$  ( $i = 1, 2$ ) and corresponding parameters for their elliptic trajectories. Hereafter we consider similar cilia that have same geometrical and dynamical properties. At micrometer scale where the dissipative effects dominate over inertial effects, the governing equations for two interacting colloidal particles (here two cilia) can be written as linear relations between the  $i$ 'th particle's velocity  $\mathbf{v}_i = \dot{\mathbf{r}}_i$  and the hydrodynamic forces acting on particles denoted by  $\mathbf{f}_j$ . In terms of their Cartesian components, we have:

$$v_{i,\mu} = \sum_{\nu=1}^3 \sum_{j=1}^2 G_{\mu\nu}(\mathbf{r}_i, \mathbf{r}_j) f_{j,\nu} \quad (1)$$

where Greek letters denote the cartesian components of the vectors. The hydrodynamic kernel  $G_{\mu\nu}$  contains information about the geometry of the system: radii of spheres, their separation and their distances to the wall. Assuming that the sphere radius,  $a$ , is much smaller than all other lengths in system, we can write an approximate form for the component of the hydrodynamic kernel in a semi infinite domain confined by a rigid wall. For  $\mathbf{r}_i \neq \mathbf{r}_j$ , we have [28]:

$$G(\mathbf{r}_i, \mathbf{r}_i) \simeq \frac{3}{2\pi\eta} \frac{z_i z_j}{d^3} \begin{pmatrix} \cos^2 \psi & \sin \psi \cos \psi & 0 \\ \sin \psi \cos \psi & \sin^2 \psi & 0 \\ 0 & 0 & 0 \end{pmatrix}, \quad (2)$$

where  $\eta$  is the fluid viscosity,  $z_i = \hat{z}_i \cdot \mathbf{r}_i$ ,  $d = \sqrt{(x_j - x_i)^2 + (y_j - y_i)^2}$  and we have assumed that  $z_i, z_j \ll d$ . Here  $\psi$  is defined as:  $\tan \psi = (y_j - y_i)/(x_j - x_i)$ . For  $\mathbf{r}_i = \mathbf{r}_j$ , we have:

$$G(\mathbf{r}_i, \mathbf{r}_i) \simeq \frac{1}{6\pi\eta a} \begin{pmatrix} 1 - \epsilon & 0 & 0 \\ 0 & 1 - \epsilon & 0 \\ 0 & 0 & 1 - 2\epsilon \end{pmatrix} \quad (3)$$

where  $\epsilon = (9a/16z)$ . Let us continue our discussion about the case of two interacting cilia near a flat wall, then we will discuss how the effects due to the curvature of the body can be considered. Denoting the inverse of hydrodynamic kernel  $G(\mathbf{r}_j - \mathbf{r}_j)$  by matrices  $M_{ij}$ , the hydrodynamic equations can be rewritten as:

$$\begin{aligned} \mathbf{f}_1 &= M_{11}\mathbf{v}_1 + M_{12}\mathbf{v}_2 \\ \mathbf{f}_2 &= M_{21}\mathbf{v}_1 + M_{22}\mathbf{v}_2. \end{aligned} \quad (4)$$

In addition to the above hydrodynamic equations, we should provide some information about the internal forces inside each cilium that drive its beating. In addition to constraining forces that enforce the particle to move on elliptic orbit, there is also tangential force that results the motion along orbit. Denoting the unit vector tangent to the trajectory of  $i$ 'th cilium by  $\mathbf{t}_i = \frac{d}{d\phi_i}\mathbf{r}_i$ , the velocity can be written as:  $\mathbf{v}_i = \dot{\phi}_i\mathbf{t}_i$ . The tangential component of the force reads as:  $f_i^t = \mathbf{t}_i^T \mathbf{f}_i$ , where symbol  $T$  denotes the transpose of a columnar matrix and we use matrix multiplication rules. In general, the tangential force is related to the velocity of sphere along its trajectory given by  $v_i^t = \hat{\mathbf{t}}_i \cdot \mathbf{v}_i$ . In linear response regime, equations like:

$$\mathbf{t}_i^T \mathbf{f}_i = f_0(1 - v_0^{-1}|\dot{\phi}_i|) \quad (5)$$

captures the dynamics of  $i$ 'th cilium. Here  $f_0$  is the stall force and it is the amount of external force necessary to stop the motion of a beating cilium. A free cilium that is not affected by any external force, moves with velocity  $v_0$ . In this linear response approximation, two parameters  $f_0$  and  $v_0$  are related to the microscopic details of the cilium. For a typical cilium,  $f_0 \sim 10\text{pN}$ ,  $a \sim 10\mu\text{m}$  and  $v_0 \sim 100\mu\text{ms}^{-1}$  [29, 30]. Using this numerical values, one can have an estimate for the stiffness of the cilium that is defined by:  $\kappa = f_0/6\pi\eta av_0 \sim 1$ . This stiffness is the only dimensionless parameter that determines the state of motion for a cilium.

Using equations 4 and 5, we can arrive at the following coupled equations for the phase variables:

$$\begin{aligned} \dot{\phi}_1 (\mathbf{t}_1^T M_{11}\mathbf{t}_1 + (f_0/v_0)|\mathbf{t}_1|) + \dot{\phi}_2 \mathbf{t}_1^T M_{12}\mathbf{t}_2 &= f_0 \\ \dot{\phi}_1 \mathbf{t}_2^T M_{21}\mathbf{t}_1 + \dot{\phi}_2 (\mathbf{t}_2^T M_{22}\mathbf{t}_2 + (f_0/v_0)|\mathbf{t}_2|) &= f_0. \end{aligned}$$

Solving these equations, one can reach to equations that reveals the dynamics of phases for two cilia case.

Let us now explain how can we take into account the curvature effects. In order to study the curvature, the hydrodynamic kernel should be replaced. In a confined

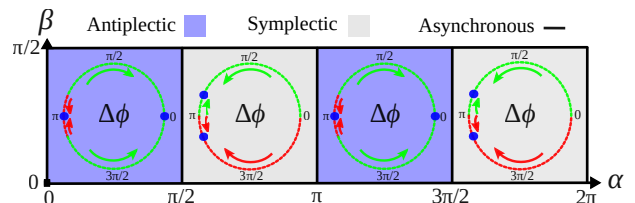


FIG. 2. Phase diagram for the state of synchronization for two or many cilia. Synchronization of two cilia depends on initial phase difference  $\Delta\phi(0)$  and  $\alpha$ . Different values of  $\Delta\phi(0)$  are shown by points on a unit circle. The synchronized states of two cilia are represented by the long time value of their phase differences,  $\Delta\phi(\infty)$ , and are shown by bolded dots on the circles. Arrows show the direction of phase evolution from initial values toward their final synchronized state, different colors are used to show the evolution to different final states. For many cilia, both symplectic and antiplectic waves can emerge. For any  $\beta \neq 0$ , antiplectic (symplectic) waves emerge for  $0 < \alpha < \pi/2$  and  $\pi < \alpha < 3\pi/2$  ( $\pi/2 < \alpha < \pi$  and  $3\pi/2 < \alpha < 2\pi$ ). Numerical parameters are:  $a/h = 0.2$ ,  $h/\ell = 0.19$ ,  $B/\ell = 0.19$ ,  $\beta = \pi/4$  and  $e = 0.87$ .

space that is limited by a curved wall, the above mentioned kernel  $G$  and subsequently its inverse given by matrix  $M$  is no longer valid. We proceed by an approximate scheme to consider the curvature effects. Here we assume that for two interacting cilia, there is an effective plane that can be used for constructing the image system. This effective wall, is a wall that is locally tangent to the curved body at the mid point of two cilia. We can use the results of flat-wall confinement, to obtain the approximate interaction between two adjacent cilia. It is obvious that with this approximation, we do not expect to see any curvature effect in the motion of two cilia. This approximation can only include non trivial curvature effects to the motion of many cilia (more than two), attached to the cylinder and it allows us to develop a consistent way for applying closed boundary condition. This approximation is valid for the case where the radius of curvature is larger than all other length scales in the system namely  $R \gg \ell$  and  $R \gg h$ .

To obtain the dynamics of two coupled cilia, one should note that in a way that we have parametrized the orbits, the kinematics of each cilium can be expressed by a single phase denoted by  $\phi_i(t)$ . This phase variable is shown in fig. 1. Solving the dynamical equations and applying the geometrical and dynamical constraints, we will arrive at the following equations [17]:

$$\dot{\phi}_i(t) = g_1(\phi_i)\omega_0 + g_2(\phi_i, \phi_j). \quad (6)$$

Here  $\omega_0 = f_0/(6\pi\eta aB(1 + \kappa))$  and the interaction between cilia are reflected by function  $g_2$  that couples the dynamics of phases. It is not possible to present analytical closed relations for functions  $g_1$  and  $g_2$  but, in principle we are able to evaluate and study them numerically. In the next section, we will summarize the results of numerical investigations of the above equations.

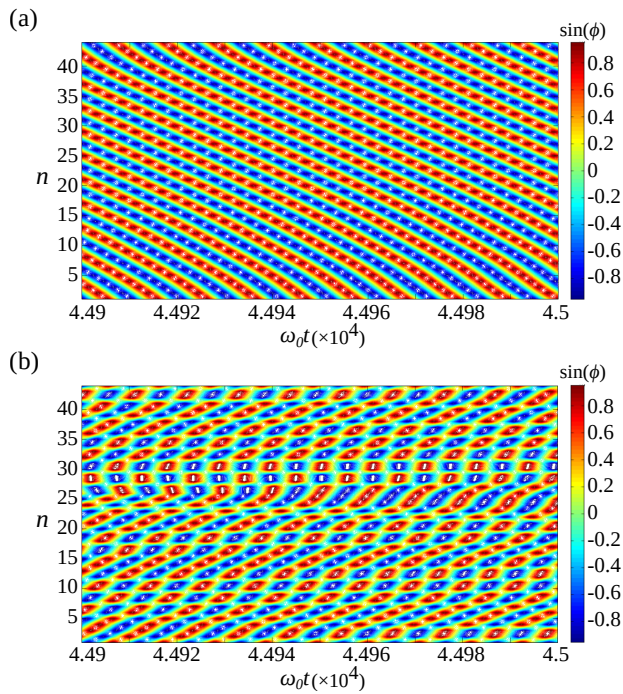


FIG. 3. State of synchronization in a collection of cilia can be seen in a time-phase portrait. The vertical axes shows the cilium number  $n$ , the horizontal axis show the time and the value of  $\sin(\phi_n(t))$  are encoded via colors. Symplectic wave appears for  $\alpha = 2\pi - \frac{\pi}{4}$  (a) and antiplectic wave appear for  $\alpha = \frac{\pi}{4}$  (b). The numerical parameters are  $a/h = 0.2$ ,  $h/\ell = 0.35$ ,  $B/\ell = 0.22$ ,  $e = 0.87$  and  $\beta = \pi/4$ .

#### IV. RESULTS AND DISCUSSION

Before studying the wave propagation in ciliated curved body, we consider the dynamics of two coupled cilia. Recalling the geometry of elliptic orbits, angles  $\alpha$  and  $\beta$ , play important role in the dynamics of coupled cilia. Numerical solutions to the equations for two interacting cilia, show that for  $\beta = 0$  and  $\beta = \pi/2$  (orbits are parallel and perpendicular to the wall respectively), the long time dynamics of cilia does not show any correlations in their beating patterns. In this case, the hydrodynamic mediated interactions between two cilia, act in an incoherent way and the state of motion for each cilium is independent from the other. This result is consistent with previous works of beating cilia near a flat wall [31, 32]. When elliptic orbits are tilted ( $\beta \neq 0, \pi/2$ ), temporal correlations in the long time dynamics of interacting cilia will appear. Our numerical studies show that for tilted orbits, the cilia reach a phase-locked synchronized state. At this synchronized state, the phase difference  $\Delta\phi(t) = \phi_2(t) - \phi_1(t)$  reaches a constant value that we will denote it by  $\Delta\phi(\infty)$ . The steady state phase difference,  $\Delta\phi(\infty)$ , depends on initial conditions, the angle of ellipse  $\alpha$  and also  $e$ . Fig. 2, shows the state of synchronization and its dependence to  $\alpha$ ,  $\beta$  and  $\Delta\phi(0)$  for  $e \neq 0$  ( $e = 0.87$ ). As one can see from this figure, for

$0 < \alpha < \pi/2$  and  $\pi < \alpha < 3\pi/2$ , depending on the initial phase difference between cilia, the final state can be either  $\Delta\phi(\infty) = 0$  or  $\Delta\phi(\infty) = \pi$ . Behavior for other values of  $\alpha$  and its sensitivity to the initial phase difference can be seen at the figure. For  $\pi/2 < \alpha < \pi$  and  $3\pi/2 < \alpha < 2\pi$ ,  $\Delta\phi(\infty)$  approaches to a constant value,  $\pi + \delta$ , where depending on the initial phase difference,  $\delta$  could be also a positive or negative small angle. The angle  $\delta$  depends on  $\alpha$ , as an example for  $\alpha = -\pi/4$ , it reaches to  $\pi/6$ . The synchronization picture shown in fig. 2, is valid for any  $e \neq 0$ . For a special case of  $e = 0$  where, the orbits are circular, and for  $0 < \alpha < \pi/2$  and  $\pi < \alpha < 3\pi/2$ , we observed that the two cilia system reaches a synchronized state with  $\Delta\phi(\infty) = 0$ . When  $e = 0$  and for  $\pi/2 < \alpha < \pi$  and  $3\pi/2 < \alpha < 2\pi$ , the systems reaches a state with  $\Delta\phi(\infty) = \pi$ .

Let us examine the dynamics of a one dimensional array of  $\mathcal{N} = 44$  cilia, attached to the circumference of a cylinder. We take into account the hydrodynamic interactions and considered both cases of elliptic and circular orbits separately ( $e = 0$  and  $e = 0.87$ ). Interestingly, unlike the case of two cilia, the emergence of synchronized states, does not show any dependence on the value of  $e$ . Fig. 3, shows two examples for the time evolution of the phase variables for all cilia. The phase values are encoded via colors. The patterns shown in this figure, demonstrate the long time dynamics of the system. The regularity of the long time patterns, reflects the temporal correlations in the motion of cilia. In this case, a traveling metachronal wave, shows a synchronized state of the cilia [9, 30, 32]. For a propagating wave (metachronal wave) in the array of cilia, the phase of  $n$ 'th cilium  $\phi_n(t)$  can be written as:  $\phi_n(t) = nK - \Omega t$ , where the number  $K$  plays the role of a wave number associated with metachronal wave. In a regular patterns shown in fig. 3, the regions with constant phases (same colors) make straight lines. These straight lines are given by an equation like:  $nK = \Omega t + C$ , where  $C$  is a constant. The slope of these parallel lines, measures the wavelength of a metachronal wave and it is given by  $1/K = \partial n / \partial(\Omega t)$ . For  $K > 0$ , the wave moves in a direction with increasing cilium's number  $n$ . As shown in fig. 1, the flow direction is always points to the left (from large  $n$  to small  $n$  cilia). So we conclude that, positive slope corresponds to antiplectic and negative slope shows a symplectic metachronal wave. Fig. 3, show two example of metachronal waves for  $\alpha = \pi/4$  and  $\alpha = 2\pi - \pi/4$ . As one can see, in the first case (fig. 3(up)), a symplectic wave has appeared, and for the second case (fig. 3(down)), an antiplectic wave has appeared. Results of our numerical investigations for the synchronization of an ensemble of cilia are shown in fig. 2. Results show that, the emergence of such synchronized states (symplectic and antiplectic), crucially depends on the value of  $\alpha$ . Independent of the value of  $e$ , the antiplectic metachronal waves appear for  $0 < \alpha < \pi/2$  and  $\pi < \alpha < 3\pi/2$ . On the other hand, symplectic metachronal waves appear when  $\pi/2 < \alpha < \pi$  and  $3\pi/2 < \alpha < 2\pi$ . Changing  $\alpha$  to  $2\pi - \alpha$ , the average

direction of the fluid flow does not change but the propagation direction of the metachronal wave will change. Comparing the results for an array of cilia with the results of two cilia, one can see that the emergence of symplectic or antiplectic synchronization in an array of cilia, is directly related to the state of synchronization in the case of two cilia. It is interesting that the antiplectic wave accompany many defects in their structures. Such defected waves have been seen in a chain of model cilia [14].

In conclusion, the state of synchronization is studied for interacting cilia. For two cilia, the synchronized state depends on the initial phase difference and the geometrical parameters of the trajectories given by  $\alpha$  and  $\beta$ . In-

phase, anti-phase ( $\delta\phi = 0, \pi$ ) synchronized states have been observed. For a  $1 - D$  array of cilia attached to a curved body, we found that, both symplectic and antiplectic metachronal waves can appear. The emergence of symplectic and antiplectic waves in an array of cilia, is in direct connection with the state of synchronization in two cilia case. As a result of our study, we understand the the geometrical characteristics are key elements in determining the state of metachronal waves. The emergence of symplectic or antiplectic metachronism in our model is not an artifact of imposing closed boundary condition. The boundary condition in our system, emerges naturally from the closed structure of the curved body.

- 
- [1] B. Alberts, A. Johnson, J. Lewis, K. Roberts, M. Raff, and P. Walter, *Molecular Biology of the Cell*, Molecular Biology of the Cell (Garland Science, 2002).
- [2] J. Blake, *Journal of Fluid Mechanics* **46**, 199 (1971).
- [3] A. Dummer, C. Poelma, M. C. DeRuiter, M.-J. T. Goumans, and B. P. Hierck, *Cilia* **5**, 1 (2016).
- [4] D. B. Hill, V. Swaminathan, A. Estes, J. Cribb, E. T. O'Brien, C. W. Davis, and R. Superfine, *Biophysical Journal* **98**, 57 (2010).
- [5] G. Witzany and M. Nowacki, *Biocommunication of ciliates* (Springer, 2016).
- [6] C. Brennen and H. Winet, *Annual Review of Fluid Mechanics* **9**, 339 (1977).
- [7] I. H. Riedel-Kruse, A. Hilfinger, J. Howard, and F. Jülicher, *HFSP journal* **1**, 192 (2007).
- [8] E. Knight-Jones, *Quarterly Journal of Microscopical Science* **3**, 503 (1954).
- [9] S. Gueron and K. Levit-Gurevich, *Biophysical Journal* **74**, 1658 (1998).
- [10] M. Lighthill, *Communications on Pure and Applied Mathematics* **5**, 109 (1952).
- [11] A. Najafi and R. Golestanian, *EPL (Europhysics Letters)* **90**, 68003 (2010).
- [12] J. Kotar, M. Leoni, B. Bassetti, M. C. Lagomarsino, and P. Cicuta, *Proceedings of the National Academy of Sciences* **107**, 7669 (2010).
- [13] R. Di Leonardo, A. Búzás, L. Kelemen, G. Vizsnyiczai, L. Oroszi, and P. Ormos, *Physical review letters* **109**, 034104 (2012).
- [14] D. R. Brumley, N. Bruot, J. Kotar, R. E. Goldstein, P. Cicuta, and M. Polin, *Phys. Rev. Fluids* **1**, 081201 (2016).
- [15] D. R. Brumley, K. Y. Wan, M. Polin, and R. E. Goldstein, *Elife* **3**, e02750 (2014).
- [16] K. Y. Wan and R. E. Goldstein, *Proceedings of the National Academy of Sciences* **113**, E2784 (2016), <http://www.pnas.org/content/113/20/E2784.full.pdf>.
- [17] A. Vilfan and F. Jülicher, *Phys. Rev. Lett.* **96**, 058102 (2006).
- [18] N. Uchida and R. Golestanian, *Physical Review Letters* **106**, 058104 (2011).
- [19] H. Stark and M. Reichert, *Journal of Biomechanics* **39**, S349 (2006).
- [20] J. Elgeti and G. Gompper, *Proceedings of the National Academy of Sciences* **110**, 4470 (2013).
- [21] D. R. Brumley, M. Polin, T. J. Pedley, and R. E. Goldstein, *Journal of The Royal Society Interface* **12** (2015), 10.1098/rsif.2014.1358.
- [22] B. Qian, H. Jiang, D. A. Gagnon, K. S. Breuer, and T. R. Powers, *Physical Review E* **80**, 061919 (2009).
- [23] R. Golestanian, J. M. Yeomans, and N. Uchida, *Soft Matter* **7**, 3074 (2011).
- [24] S. H. Rad and A. Najafi, *Physical Review E* **82**, 036305 (2010).
- [25] B. Nasouri and G. J. Elfring, *Phys. Rev. E* **93**, 033111 (2016).
- [26] P. Lenz and A. Ryskin, *Physical Biology* **3**, 285 (2006).
- [27] B. Guirao and J.-F. Joanny, *Biophysical journal* **92**, 1900 (2007).
- [28] C. Pozrikidis, *Boundary integral and singularity methods for linearized viscous flow* (Cambridge University Press, 1992).
- [29] J. Howard, *Mechanics of Motor Proteins and the Cytoskeleton* (Sinauer Associates, Publishers, 2001).
- [30] D. R. Brumley, M. Polin, T. J. Pedley, and R. E. Goldstein, *Phys. Rev. Lett.* **109**, 268102 (2012).
- [31] P. Lenz and A. Ryskin, *Physical Biology* **3**, 285 (2006).
- [32] T. Niedermayer, B. Eckhardt, and P. Lenz, *Chaos: An Interdisciplinary Journal of Nonlinear Science* **18**, 037128 (2008).